An Analysis of the Asymptotic Limit of Gluon Shadowing.

S. Liuti [a] * and F. Cano [b]

[a] *Institute of Nuclear and Particle Physics, University of Virginia, McCormick Road, Charlottesville, Virginia 22901, USA.*

[b] *Dipartmento di Fisica, Universitá di Trento, Via Sommarive 14, 38050 Povo, Trento, Italy.*

Abstract

We examine the gluon distributions in nuclei in the asymptotic region defined by $Q^2 \to \infty$, $x \to 0$. An analysis using the Double Asymptotic Scaling variables of Ball and Forte is proposed. New scaling relations are predicted which can help disentangling the different mechanisms of low x perturbative QCD evolution in nuclei.

Submitted to Physics Letters B

Typeset using REVTEX

*On leave from: INFN-Sezione Roma Tre, Dipartimento di Fisica E. Amaldi, Via Vasca Navale, 84. 00146 Roma, Italy.

1. Nuclear shadowing or the depletion at low Bjorken x of the nuclear Deep Inelastic (DI) structure function, F_2^A, with respect to the nucleon one, F_2^N, has been observed in a number of experiments ([1] and references therein). Assuming the universality of parton distributions in nuclei, one expects nuclear shadowing to be present in other high energy processes as well, such as Drell-Yan pair, J/ψ and Υ production in lepton-nucleus, hadron-nucleus and nucleus-nucleus collisions ([2] and references therein). In particular nuclear shadowing might be concurring with the other mechanisms, among which is the quark-gluon plasma formation, that result in a depletion of the observed cross sections for these processes. Moreover, as the very low x regime has become accessible at HERA, new phenomenological studies of high density QCD at the saturation scale predicted in [3] are now possible [4]. A quantitative understanding of both the x and Q^2 dependences of the nuclear parton distributions at low x therefore constitutes a practical and necessary step both for interpreting the outcome of future experiments at RHIC and at the LHC and for investigating the onset of parton saturation.

Recent calculations rely on non-perturbative models for the nuclear parton distributions at a given (low) scale, Q_o^2, combined with DGLAP [5] perturbative evolution. They are all therefore affected by the uncertainty in the initial parton distributions and, in particular, in the gluon distribution which governs evolution at low x, and which is poorly known experimentally. A strong effect is seen by changing the value of Q_o^2 itself which can plausibly vary within the range, $Q_o^2 = 0.8 - few\,\mathrm{GeV}^2$, leading to sensibly different values for the shadowing of both the structure function and the gluon distribution at large Q^2.

Now, as Q^2 increases the (low x) gluon distribution in a proton should tend to a universal asymptotic value, corresponding to the Double Leading Logarithmic Approximation (DLLA) result of Ref. [6]. Numerically, this value is attained at $Q^2 \lesssim 10^3\,\mathrm{GeV}^2$ provided the initial distributions grow much slower than $\approx x^{-1/2}$. Because of the coupling between the singlet quark and gluon distributions' evolution, a similar behavior is predicted for the structure function, F_2 [7]. It is therefore natural to address the question of whether the differences in the initial non perturbative nuclear shadowing will decrease with growing Q^2 and give

rise to a universal asymptotic curve which is within the range of planned experiments. Our first result is a negative one: we will show that because of the form that DGLAP evolution takes in a nucleus the influence of initial conditions is carried on to the largest attainable Q^2 values.

We then examine carefully the asymptotic behavior of the shadowing ratios $R_G = G_A/G_N$ and $R_F = F_2^A/F_2^N$, in the DLLA (notations are: $G_{N(A)}$ and $F_2^{N(A)}$ for the gluon distributions and the structure function in a nucleon, (N), and in an isoscalar nucleus, (A), respectively). Our goal is to ascertain whether it is possible to distinguish among the different approximations the perturbation series takes in a nucleus and at very low x.

The proton structure function data analyzed recently at HERA [8,9] have been shown [8] to lie in the asymptotic region ($Q^2 \gg Q_o^2 = 1\,\mathrm{GeV}^2$ and $x \ll x_o = 0.1$, and to evolve according to DLLA [10]. The key test is to prove that the data obey Double Asymtptotic Scaling (DAS) in the variables $\rho = \gamma((Y - Y_o)/\xi)^{1/2}$ and $\sigma = \gamma^{-1}((Y - Y_o)\xi)^{1/2}$, $\gamma = 6/(33 - 2N_f)^{1/2}$, $Y = \ln 1/x$, $\xi = \gamma^2 \ln(\ln Q^2/\Lambda_{QCD}^2/\ln Q_o^2/\Lambda_{QCD}^2)$. Violations from DAS (other than due to the fact that the data lie in a pre-asymptotic region [10]) would signal either the onset of contributions beyond standard pQCD evolution [5], including the beginning of parton saturation [3,4].

The approach to asymptotia in a nucleus can be first analyzed by assuming that evolution proceeds through DLLA equations as well. We have found that in this case the ratios R_F and R_G display exact scaling in σ, thus becoming a function of ρ only. As in the proton case, this is a model independent result in that we obtain a scaling form, independent from the initial conditions. We then use this result as a basis for addressing the next question *i.e.* the detection of violations of DAS scaling in nuclei, which could possibly originate at different values of $x \equiv x_o^A$ and $Q^2 \equiv Q_{o,A}^2$, than in the proton. In particular Unitarity Shadowing Corrections (USC) [11,12,24] are expected to affect evolution at $x_o^A > x_o$ because of the increase of the tranverse gluon density in a nucleus due to the overlapping of nucleons in the longitudinal direction. On a more speculative basis one might also expect the transition to the $\ln(1/x)$ resummation to appear in a different regime or, in the most "exotic" scenario,

that medium modifications of the anomalous dimensions could be observed. In our approach such questions can be addressed systematically as they introduce specific *scaling violations* from the DLLA result, appearing as different σ dependences in the ratios R_G and R_F.

Our main observation is therefore that although it is technically predictable that for a proton target DGLAP evolution and DLLA should break down at very low values of x and sufficiently large Q^2 and give way to $\ln(1/x)$ summation and to USC, it is still a major task to be able to pinpoint where and if the transition from the different regimes is going to take place in the kinematical regimes currently under exploration. Our goal is to obtain some new insight by using nuclear targets where the asymptotic regime can in principle be reached at larger x. As a by-product we obtain quantitative predictions in the asymptotic kinematic regime which should be attainable at RHIC and at the LHC.

2. We first summarize results for ordinary DGLAP evolution applied to the nuclear ratios at low x, assuming that the proton and the nuclear distributions evolve similarly. As it is well known evolution is driven by the gluon distribution which dominates over the sea quarks one and one can predict the behavior of the shadowing ratios, R_G and R_F with Q^2:

$$\frac{\partial R_G}{\partial \ln Q^2} \simeq \int_x^1 P_{GG}\left(\frac{x}{y},\alpha_S(Q^2)\right)\frac{G_N(y,Q^2)}{G_N(x,Q^2)}\left[R_G(y,Q^2)-R_G(x,Q^2)\right]\frac{dy}{y}$$
$$\equiv \frac{\partial G_N/\partial Q^2}{G_N}\left(\frac{\partial G_A(x,Q^2)/\partial \ln Q^2}{\partial G_N(x,Q^2)/\partial \ln Q^2}-R_G(x,Q^2)\right), \qquad (1)$$

$$\frac{\partial R_F}{\partial \ln Q^2} \simeq \int_x^1 P_{qG}\left(\frac{x}{y},\alpha_S(Q^2)\right)\frac{G_N(y,Q^2)}{\Sigma_N(x,Q^2)}\left[R_G(y,Q^2)-R_F(x,Q^2)\right]\frac{dy}{y}, \qquad (2)$$

where we have disregarded the sea quarks distribution on the *r.h.s.* of the coupled DGLAP evolution equations; P_{qG} and P_{GG} are the splitting functions evaluated at NLO; and we used the approximation $F_2^{N(A)} \approx 5/18\Sigma_{N(A)}$, with $\Sigma = \sum_i q_i(x,Q^2)+\bar{q}_i(x,Q^2)$. For ease of presentation we will use the following notation: $G'_{N(A)} = \partial G_{N(A)}(x,Q^2)/\partial \ln Q^2$. Eqs.(1) and (2) show that the Q^2 dependence of the ratios R_G and R_F is determined by a subtle balance involving both the parton distributions and the ratios themselves [14]. Based on Eqs.(1) and (2), and defining $R_G(x,Q_o^2) \equiv R_G^o$ and $R_F(x,Q_o^2) \equiv R_F^o$ for the initial distributions, one

can make the following predictions for the Q^2 dependence of R_G and R_F: *i)* R_G grows with Q^2. In fact, if as predicted by non-perturbative shadowing models R_G is a growing function of x, then it also grows with Q^2, the *r.h.s.* of Eq.(1) being positive ($y \geq x$); *ii)* if $R_F^o < R_G^o$, then R_F grows with Q^2; if $R_F^o > R_G^o$, then R_F initially decreases with Q^2 until it reaches the value of R_G^o and it subsequently starts increasing along with R_G.

Note that from the behavior of R_F and R_G obtained from the straighforward application of DGLAP equations, one cannot predict the approach of *e.g.* R_G to a universal limiting curve at large Q^2. As a matter of fact, although the form of Eq.(1) might seem suggestive of a fixed point behavior [15], this is *a priori* not the case, since the quantity $G_A\prime/G_N\prime$ depends on Q^2. The rate of change with Q^2 is instead governed both by: (a) by the ratio, G'_N/G_N; (b) by the difference $\Delta_G = G'_A/G'_N - R_G(x,Q^2)$ at $Q^2 = Q_o^2$. Current parametrizations [16,17] feature an ultra-soft behavior of the gluon distribution at $Q_o^2 \leq 1\,\mathrm{GeV}^2$, *i.e.* $G_N \rightarrow 0$ as $x \rightarrow 0$, thus causing (because of (a)) a rapid evolution which strongly reduces the shadowing in both R_G and R_F, between Q_o^2 and $Q^2 \approx 1 - 2\,\mathrm{GeV}^2$. If on the contrary one assumes Q_o^2 ranging from 2 to $5\,\mathrm{GeV}^2$, where harder low x initial gluons are expected, then the evolution is slower (G_N is larger) and the nuclear ratio is basically unchanged at $Q^2 \approx 10 - 100\,\mathrm{GeV}^2$. A further model dependence follows from the usage of different non-perturbative shadowing mechanisms. We examine two in particular: the Aligned Jet Model (AJM) (see [18] and references therein), and Initial State Recombination (ISR) [19]. Both models explain qualitatively the initial onset of shadowing. Accurate quantitative calculations have been performed using the AJM in [20,21].

Results are summarized in Fig.1, where we show the Q^2 dependence of the ratios $R_F(x,Q^2)$ and $R_G(x,Q^2)$ in ^{40}Ca at fixed $x = 10^{-4}$ (Fig. 1(a)) and $x = 10^{-2}$ (Fig. 1(b)), for both the AJM (full lines) and the ISR model (short dashes). In order to show the dependence on the initial scale Q_0^2, results are presented for both models by taking, $Q_0^2 = 0.8$ GeV^2, and $Q_0^2 = 5$ GeV^2 (the latter can be easily distinguished in the graph by observing the shift in the starting point of the curves). Moreover, as the main purpose of the figure is to illustrate the main features of both the nuclear models and the initial parton distributions

that will lead to our description on the asymptotic behavior, we have not sought for R_F the best agreement with the data. Details on this part are going to be given elsewhere [22]. A remarkable feature is the sensitivity of the ISR model to this initial scale Q_0^2. It is only for $Q_0^2 \lesssim 1$ GeV^2 that a sizeable gluon shadowing is obtained due to the fact that the amount of initial shadowing is proportional to the square of the initial gluon distributions and to $\alpha_s(Q_0^2)/Q_0^2$ [19]. Results obtaind with the AJM vary less dramatically with the initial scale, Q_0^2, which in this case enters just the $(q\bar{q}) - nucleon$ (or $(gg) - nucleon$) cross sections [18]. Nonetheless, the initial difference is carried on to Q^2 as large as 10^3 GeV^2. Moreover, in both cases we can observe the Q^2 behaviour outlined before: a rapid suppression of shadowing in the range of Q^2 up to 2 GeV^2 and a subsequent softer evolution. The comparison between the Q^2 behaviour for different fixed x values (Fig. 1(a) and Fig. 1(b)) shows that evolution is slower for smaller x. This can be technically understood by noting that, in the DLLA limit the logarithmic derivative of R_G in Eq. (1) vanishes. This is why initial discrepancies between models are more likely to persist at smaller x.

In summary, the asymptotic behavior of R_G depends on the initial conditions up to the largest values of Q^2 attainable at low x. This feature is in common with the proton gluon distributions themselves as shown *e.g.* in [7]. As it is well known, neither the data nor theoretical arguments can help us defining the optimal values of $R_G(x, Q_o^2)$ and $R_F(x, Q_o^2)$.

The situation that we have described calls for some redefinition of the approach to asymptotia in deep inelastic scattering from nuclei. In the next Section we illustrate how different behaviors of the data could be revealed by extending the double asymptotic scaling analysis of Ref. [10] to nuclei.

3. We now examine the nuclear DI structure function and gluon distribution in the asymptotic regime defined by $x \to 0$, $Q^2 \to \infty$. Our goal is to explore scaling relations in nuclei in order to be able to compare theory with data in a model independent way. The derivation of the equations of the DLLA in a nucleus parallels the one for the proton, namely one first writes the DGLAP evolution equation for the gluon distribution in the limit $n \to 1$, n being the variable in moments space (we have omitted the subscripts $N(A)$ unless

necessary):

$$\frac{\partial g(n,Q^2)}{\partial \ln Q^2} = \frac{\alpha_s(Q^2)}{2\pi}\gamma^0_{GG}(n) g(n,Q^2), \tag{3}$$

$\gamma^0_{gg}(n) \approx 2C_A/(n-1) + \kappa$ being the anomalous dimension in the limit $n \to 1$ ($\kappa = -11/6 - n_f/3C_A$ is the next-order or subleading contribution in this limit). Solutions in (x, Q^2) are found by evaluating the anti-Mellin transform,

$$G(x,Q^2) = \frac{1}{2\pi i}\int_C dn\, g(n,Q^2)\exp\left[Y(n-1)\right], \tag{4}$$

with the saddle point method [6]. In Eq.(4), $g(n,Q^2) = g(n,Q_0^2)\exp\left[\xi/(n-1) + \xi\kappa/2\right]$; $g(n,Q_0^2) = \int_0^1 dx\, x^{(n-1)} g(x,Q_0^2)$, $g(x,Q_o^2)$ being the initial gluon distribution, and $G(x,Q^2) = xg(x,Q^2)$; $Y = \ln(1/x)$, and $\xi = \gamma^2 \ln(\ln(Q^2/\Lambda^2)/(\ln Q_o^2/\Lambda^2))$, $\gamma^2 = C_A/(\pi b)$, $b = (33 - 2N_f)/12\pi$. We rewrite the integrand in Eq.(4) as:

$$\widetilde{g}(n,Q^2) = g(n,Q_o^2)\exp\xi\kappa/2\exp[Yf_1(n) + \xi f_2(n)], \tag{5}$$

where $f_1(n) = n-1$, $f_2(n) = (n-1)^{-1}$ and Y and ξ are both similarly large. If one takes "soft" initial conditions such as, $G(x,Q_0^2) \approx A_N x^{-\lambda}$, $\lambda \lesssim 0$, then $g(n,Q_0^2) \approx A_N/(n-(\lambda+1))$ has a pole to the left of the saddle point which is found by setting $\partial[Yf_1(n) + \xi f_2(n)]/\partial n = 0$. The integral in Eq.(4) is then approximated by:

$$\begin{aligned} G(x,Q^2) &= \sqrt{2\pi}\left(\frac{\widetilde{g}(n_o,Q_o^2)}{\widetilde{g}''(n_o,Q_o^2)}\right)^{1/2}\widetilde{g}(n_o,Q^2) = \\ &= \sqrt{2\pi}g(n_o,Q_o^2)\exp(\xi\kappa/2)\frac{\exp[Yf_1(n_o) + \xi f_2(n_o)]}{|Yf_1''(n_o) + \xi f_2''(n_o)|^{1/2}} \end{aligned} \tag{6}$$

where $n_0 = 1 + \sqrt{\xi/\Delta Y}$, $\Delta Y = Y - Y_o$, $Y_o = \ln(1/x_o)$, $x_o \approx 0.1$, is the saddle point and $f''_{1(2)}(n_o) = \partial^2 f_{1(2)}(n)/\partial n^2\Big|_{n=n_o}$.

By introducing the variables, $\rho = \gamma((Y-Y_o)/\xi)^{1/2}$ and $\sigma = \gamma^{-1}((Y-Y_o)\xi)^{1/2}$, [10] one has:

$$n_o \equiv n_o(\rho) = 1 + \gamma/\rho, \tag{7}$$

and,

$$G \equiv G^{DAS}(\rho,\sigma) = \sqrt{\pi} f_G(\rho/\gamma) \left(\frac{\gamma}{\rho}\right) \frac{\exp\left[2\gamma\sigma - \gamma^2\kappa/2\right]}{\sqrt{\sigma\gamma}}, \tag{8}$$

where $f_G(\rho/\gamma)$ is a smooth function describing the initial conditions.

DAS is the prediction that, in the hypothesis of soft initial conditions, and in the asymptotic limit defined by $\sigma \to \infty$ and $\rho \approx O(1)$, $\ln(G^{DAS}/f_G(\rho,\sigma))$ becomes a linear function of σ, independent of the value of ρ, with slope fixed by the known constant, γ.

A similar behavior is found for F_2^p [10] and can therefore be compared to the available data [8,9]. The structure function's asymptotic behavior is in fact obtained by solving the equation [1]:

$$\frac{\partial F_2^p(x,Q^2)}{\partial \ln Q^2} = \frac{5}{18}\frac{\alpha_S}{\pi} G(x,Q^2), \tag{9}$$

yielding:

$$F_2^p(\rho,\sigma) = f_\Sigma(\rho,\sigma)\exp(2\gamma\sigma), \tag{10}$$

where f_Σ was derived by using the LO expression for α_s and, as for the gluons, it depends on the initial conditions. The scaling of F_2^p can be seen from Fig.2 (top-right). From Fig.2 one can also see that the data from NMC (triangles) [23], corresponding to larger x with respect to the 1995 HERA ones (open squares) [8], as well as some of the more recent HERA data with very low x and Q^2 (open dots) [9], violate scaling (for a better reading compare with top-left). These scaling violations have been interpreted as due to the fact that the kinematics is not yet asymptotic, as it can be easily seen from the fact that the data lie well below $\sigma \approx 1$.

Deviations from DAS can be predicted also in the case of hard initial conditions *i.e.* when $g(n_0,Q_0^2) \approx A_N/(n-(\lambda+1))$ with $\lambda \gtrsim 0.2$. Intuitively this corresponds to taking the limit $Y \gg \xi$ in Eq.(4), thus defining the new saddle point: $n_o = (1+\lambda) + 1/\Delta Y$. The corresponding gluon distribution is then

[1] We refer here to the singlet part of the structure function

$$G(x,Q^2) = f_G^h \exp\left[\lambda(Y-Y_o) + \xi/\lambda + \xi\kappa/2\right]$$
$$= f_G^h \exp\left[\lambda\sigma\rho + (\gamma^2/\lambda + \kappa/2)\xi\right] \quad (11)$$

with $f_G^h(\rho,\sigma) = \sqrt{2\pi\rho\sigma}A_N$ (see also [13]). This behavior supports the presence of USC appearing as a non-linear term in the evolution equation [11], which has the effect of damping the steep rise of the gluon distribution at small x. An alternative possible explanation of DAS violations in the recent HERA data [9] which accounts also for the peculiar stooping of the logarithmic slope of the proton structure function, $\partial F_2/\partial \ln Q^2$, at low x and Q^2, is that indeed USC [24] need to be taken into account.

We now study these two different scenarios for the asymptotic behavior in nuclei, where it is well known that some aspects of perturbative evolution such as USC, are expected (simply based on geometrical arguments) to arise at larger values of x. In Fig.2 we present the world low x data on the nuclear ratios, Eq.(1) as a function of the DAS variable, σ (bottom-right), and we compare both data and their kinematics (bottom-left) with the proton ones (top). We use in both cases the following values of Q_o^2, Λ_{QCD}, ρ and σ: $Q_o^2 = 1\,\mathrm{GeV}^2$, $\Lambda_{QCD} = 185$ MeV (LO). [2] From the figure it appears that the existing nuclear data are scarse and do not presently support a DAS type analysis and, moreover, they seem to lie mainly in a pre-asymptotic region. Experiments at RHIC and LHC are however expected to be able to cover the asymptotic region. Although experimental extractions of the logarithmic slopes in nuclei have been performed in [1], very little can be concluded from these data as well [22].

We evaluate the ratios R_G and R_F, Eq.(1) in DAS, *i.e.* within the hypotheses: *i)* the quark and gluon distributions are initially shadowed due to some non-perturbative mechanism; *ii)* the pQCD evolution mechanism is not affected by the nuclear medium; *iii)* the initial distributions are soft. The DLLA predictions are:

$$R_G(x,Q^2) = \left[\frac{\widetilde{g}_A(n_o,Q^2)}{\widetilde{g}_N(n_o,Q^2)}\right]^{3/2} \left[\frac{\widetilde{g}'_N(n_o,Q^2)}{\widetilde{g}'_A(n_o,Q^2)}\right]^{1/2}, \quad (12)$$

[2] In the NLO analysis performed in [10] it was found that: $Q_o^2 = 1.8\,\mathrm{GeV}^2$, $\Lambda_{QCD} = 200$ MeV (NLO), $\rho \approx 1$ and $\sigma \gtrsim 1.2$.

where n_o is the saddle point defined by Eq.(7) for both the proton and the nucleus We rewrite Eq.(12) as a function of the DAS variables by using Eq.(8):

$$R_G^{DAS} = \frac{f_G^A(\rho/\gamma)}{f_G^N(\rho/\gamma)} \tag{13}$$

i.e. the exponential terms appearing in $G^{DAS}(\rho,\sigma)$, Eq.(8), are the same in a nucleus and in a single nucleon respectively, thus canceling the σ dependence in the ratio R_G: R_G is predicted to scale exactly in σ to a smooth function of ρ that is determined entirely by the (soft) initial conditions.

The onset of a different evolution mechanism in the nucleus will appear as a *σ-scaling violation* modifying the exponential behavior of Eqs.(8)-(12) with respect to the single nucleon case. Since the low x behavior of recent HERA data seem to show evidence for rather large screening corrections, and at the same time they do not rule out the hard pomeron contribution, we consider the effect of: **(A)** USC combined with soft initial conditions; **(B)** USC combined with hard initial conditions; **(C)** Hard initial conditions in both nucleon and nucleus, no USC.

The effect of USC is taken into account through a "damping factor", $D_G(x,Q^2) \leq 1$, (Ref. [24] and references therein), evaluated using Mueller-Glauber's eikonal approximation [27]. We extended the calculation to nuclei by assuming that two gluons inside a nucleus are correlated by a larger confinement radius, $R_A \approx r_0 A^{1/3}$, than in a nucleon, corresponding to a smeared impact parameter space two-gluon form factor (details of this calculation will be included in [22]). As a result the effect USC is enhanced in a nucleus with respect to a nucleon target, due to the larger transverse gluon density at similar values of x.

The asymptotic gluon distribution function is written in terms of the damping factor as:

$$G_{N(A)}^{SC}(\rho,\sigma) = D_G^{N(A)} \times G^{DAS}(\rho,\sigma). \tag{14}$$

By using Eq.(14) We can now calculate the ratio R_G, for the cases listed above. We obtain:

$$R_G^{(A)}(\rho,\sigma) = R_G^{DAS}(\rho) \times \frac{\exp\left[2\gamma(\sigma-\sigma_A) - \frac{\gamma^2\kappa}{2}\frac{\sigma}{\rho}\right]}{\exp\left[2\gamma(\sigma-\sigma_N) - \frac{\gamma^2\kappa}{2}\frac{\sigma}{\rho}\right]} \equiv$$

$$\equiv R_G^{DAS}(\rho) \times \exp\left[-(\sigma_A - \sigma_N)\right]. \tag{15a}$$

$$R_G^{(B)}(\rho,\sigma) = \frac{f_G^{h,A}}{f_G^{h,N}} \times \frac{\exp\left[\lambda_A\sigma\rho + \frac{\gamma^2}{\lambda_A}\frac{\sigma}{\rho} - \sigma_A\right]}{\exp\left[\lambda_N\sigma\rho + \frac{\gamma^2}{\lambda_N}\frac{\sigma}{\rho} - \sigma_N\right]} \equiv$$

$$\equiv C\exp\left[(\lambda_A - \lambda_N)\sigma\rho + \gamma^2(\frac{1}{\lambda_A} - \frac{1}{\lambda_N})\frac{\sigma}{\rho}\right] \times \exp\left[-(\sigma_A - \sigma_N)\right]. \tag{15b}$$

$$R_G^{(C)}(\rho,\sigma) = C\exp\left[(\lambda_A - \lambda_N)\sigma\rho + \gamma^2(\frac{1}{\lambda_A} - \frac{1}{\lambda_N})\frac{\sigma}{\rho}\right]. \tag{15c}$$

Here R_G^{DAS} is the same as in Eq.(13); $\sigma_{N(A)}(\rho,\sigma) = 1/2\gamma\ln(1/D_G)$; and the shadowing for the initial hard distributions has been parametrized as $R_G^{(o)} = f_G^{h,A}/f_G^{h,N} = Cx^\alpha$, with $C \approx 1.3$ and $\alpha \approx 0.08 - 0.1$. Moreover, we have chosen $Q_o^2 = 1\,\mathrm{GeV}^2$ for both soft and hard initial conditions and $\lambda_N = 0.35$. Our scaling result, Eq.(13), and the scaling violating ones, Eqs.(15a)-(15c), are shown in Fig.3 for two different values of ρ: $\rho = 1.8$ well inside the asymptotic region shown in Fig.2, and $\rho = 3.4$ corresponding to very low x and almost fixed Q^2 where we expect standard DGLAP to break down.

A few comments are in order. Starting from soft initial conditions one obtains either the σ-scaling curves (full lines) or the σ-scaling violation, Eq.(15a), induced by USC (dashed lines). These corrections are driven by the damping factor given for each value of ρ by the dashed curves below. The decreasing trend with growing σ is larger at large ρ because of the correspondingly decreasing values of x at similar values of Q^2. On the other side, hard initial conditions, Eq.(11) and dot-dashed curves in Fig.3, show sensible deviations from σ-scaling at large ρ where the $\ln(1/x)$ term dominates over the $\ln Q^2$ one. This effect is enhanced by USC (dotted curves). An interesting observation is the change in slope of the scaling violations both when passing from soft to hard initial conditions at low ρ, and when passing from low ρ to large ρ. These and similar other regularities could be studied systematically both for the gluon and the structure function ratios once a much larger set of data will be available.

Most importantly, with the approach proposed here we eliminate the ambiguities in the determination of the value of gluons and quarks nuclear shadowing illustrated in Fig.1, in that we identify scaling relations that must be verified independently from the initial

non-perturbative nuclear shadowing.

In conclusion, by applying DAS to nuclei we have shown model independent predictions, *i.e.* scaling in the variable ρ for the ratios of the nuclear gluon distributions to the free nucleon ones in the asymptotic region. Similar relations hold for the nuclear structure functions. We have considered a few possible sources of scaling violations due to the onset of USC and to the domination of a hard pomeron. As a result, by studying the A-dependence of shadowing we find some new constraints on perturbative evolution at low x. Our calculations are relevant for the regime accessible at future experiments at RHIC, LHC and at the eA project at DESY [28].

REFERENCES

[1] M. Arneodo, Phys. Rep. **240** (1994) 301.

[2] M.J. Leitch et al., LA-UR-99-5007, nucl-ex/9909007.

[3] A.H. Mueller, Nucl.Phys. **B558** (1999) 285.

[4] S. Bondarenko, E. Gotsman, E. Levin and U. Maor, TAUP-2616-99, hep-ph/0001260.

[5] L.V. Gribov and Lipatov, Yad.Fiz. **20** (1975) 181; G. Altarelli and G. Parisi, Nucl.Phys. **B126** (1977) 298; Dokshitzer, Sov.Phys.JETP **46** (1977) 641.

[6] A. De Rujula et al., Phys. Rev. **D10** (1974) 1649.

[7] A.D. Martin, R.G. Roberts and W.J. Stirling, Phys. Rev. **D37** (1988) 1161.

[8] (a) H1 Collaboration, T.Ahmed et al., Nucl.Phys. **B439** (1995) 471; (b) C. Adloff et al., Nucl.Phys. **B497** (1997) 3; (c) S. Aid et al., Nucl.Phys. **B470** (1996), 3.

[9] ZEUS Collaboration, M. Derrick et al., Z.Phys. **C69** (1996) 607; J. Breitweg et al., Phys.Lett. **B407** (1997) 432

[10] R. Ball and S. Forte, Phys. Lett. **B335** (1994) 77; *ibid* **B336** (1994) 77; Nucl. Phys. Proc. Suppl. **54A** (1997) 163.

[11] L.V. Gribov, E.M. Levin and M.G. Ryskin, Phys. Rep. **100** (1983) 1.

[12] A.H. Mueller and J. Qiu, Nucl. Phys. **B268** (1986) 427.

[13] J.C. Collins and I. Kwiecinski, Nucl. Phys. **B335** (1990) 89.

[14] J. Qiu, Nucl. Phys. **B291** (1987) 746.

[15] Z. Huang, H.J. Lu and I. Sarcevic, Nucl. Phys. **A637** (1998) 79.

[16] A.D. Martin, R.G. Roberts, W.J. Stirling and R.S. Thorne, Eur.Phys.J. **C4** (1998) 463.

[17] M. Glück, E. Reya and A. Vogt, Eur.Phys.J. **C5** (1998) 461.

[18] L.L. Frankfurt and M.I. Strikman, Nucl. Phys. **B316** (1989) 340.

[19] F.E. Close, J. Qiu and R.G. Roberts, Phys.Rev. **D40** (1989) 2820.

[20] K. Eskola, V.J. Kolhinen and P.V. Ruuskanen, Nucl. Phys. **B535** (1998) 351.

[21] L.L. Frankfurt, M.I. Strikman and S. Liuti, Phys. Rev. Lett. **64** (1990) .

[22] F. Cano and S. Liuti, *in preparation*.

[23] NMC Collab. Phys. Lett. **B295** (1992) 159.

[24] E. Gotsman, E.Levin, U.Maor and E. Naftali, Nucl. Phys. **B539** (1999) 535.

[25] M. Arneodo et al., Nucl. Phys. **B441** (1995) 12; P. Amaudruz et al., Z. Phys. **C53** (1992) 73.

[26] M.R. Adams et al., Phys. Lett. **B287** (1992) 375; Phys. Rev. Lett. **68** (1992) 3266.

[27] A.H. Mueller, Nucl. Phys. **B335** (1990) 115.

[28] *Workshop on Physics with HERA as eA Collider*, DESY, Hamburg, 25-26 May, 1999, C99/05/95.

FIGURES

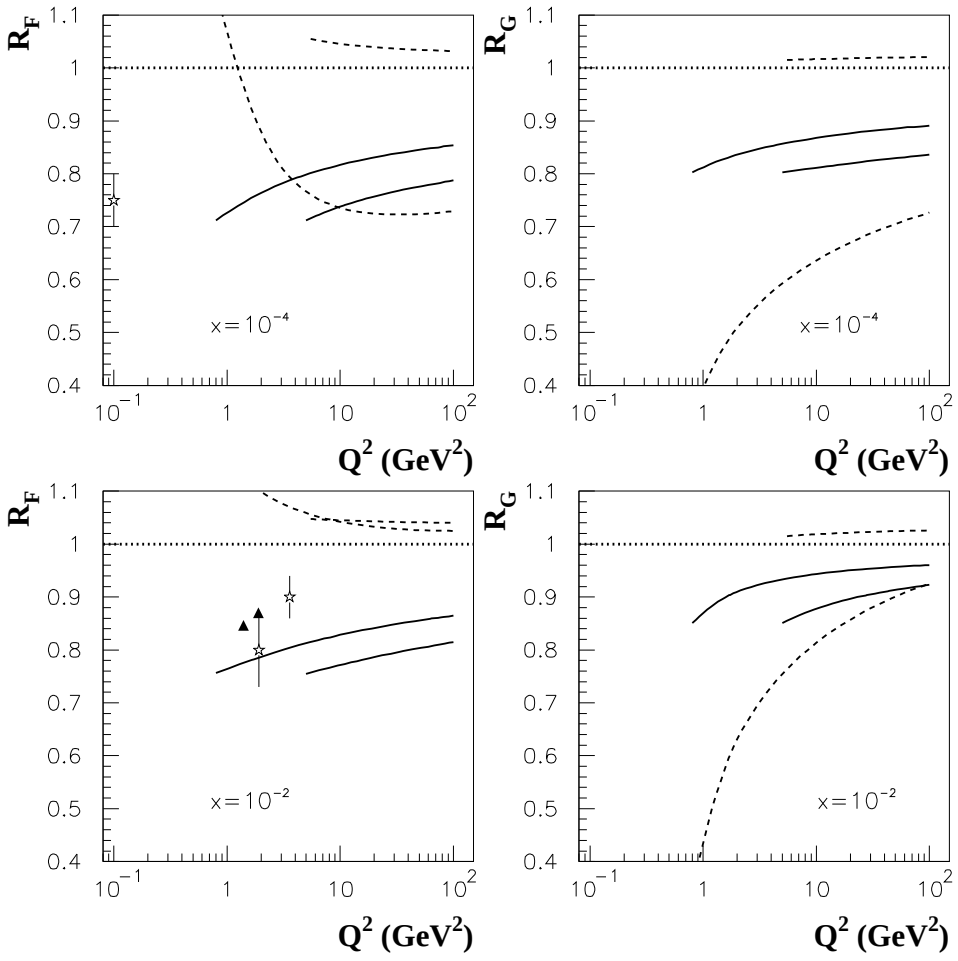

FIG. 1. DGLAP evolution in ^{40}Ca. Experimental data from NMC [25] (triangles) and E665 [26] (stars); theoretical curves are explained in the text.

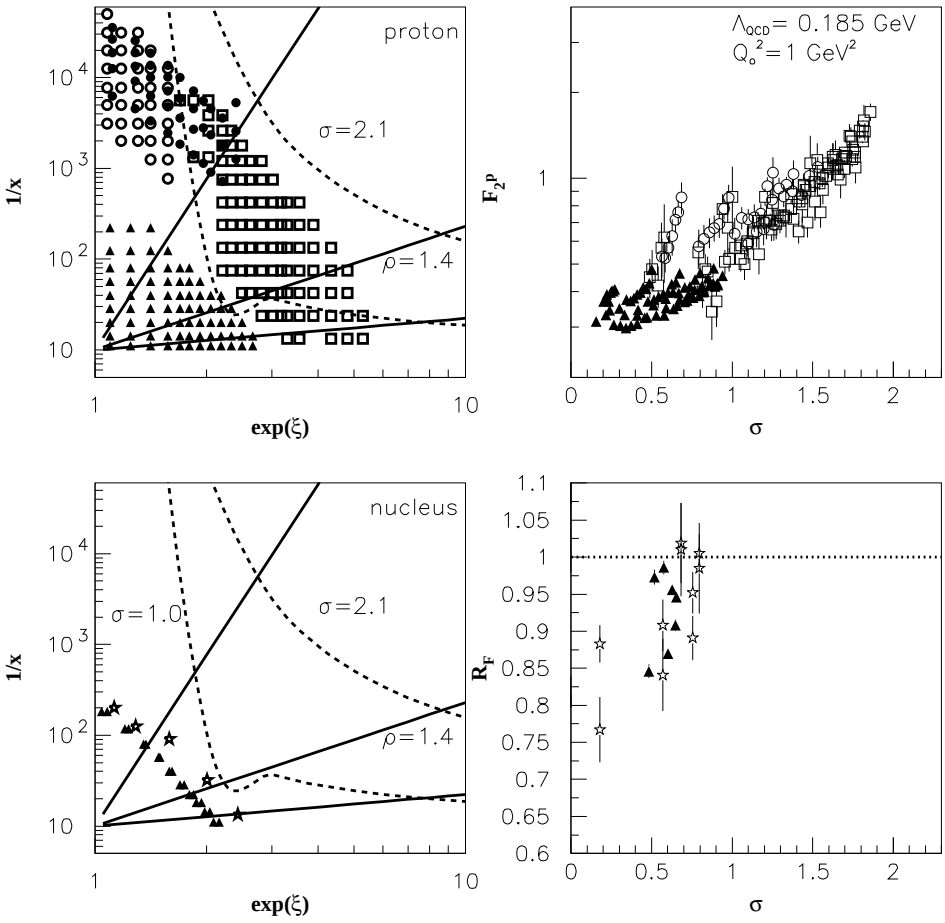

FIG. 2. The asymptotic region in the proton (top) and in a nucleus (bottom). The figures on the left show the kinematical range in $Y = 1/x$ and ξ covered by current experiments: NMC [23] [25] (triangles), H1 [8]a (squares) and [8]b,c (full dots), ZEUS [9] (open dots), E665 [26] (stars). The asymptotic region is delimited by the values: $0.7 < \rho < 3$ (full lines) and $1 < \sigma < 2.1$ (dashed lines). The figures on the right show the onset of DAS in the proton (top) and the shadowing ratio, R_F, vs. σ in a nucleus (bottom). While DAS is achieved in the asymptotic region covered mostly by the H1 [8] data, a regular pattern is yet to be seen in the nuclear data which are clearly lying outside the asymptotic region (left bottom).

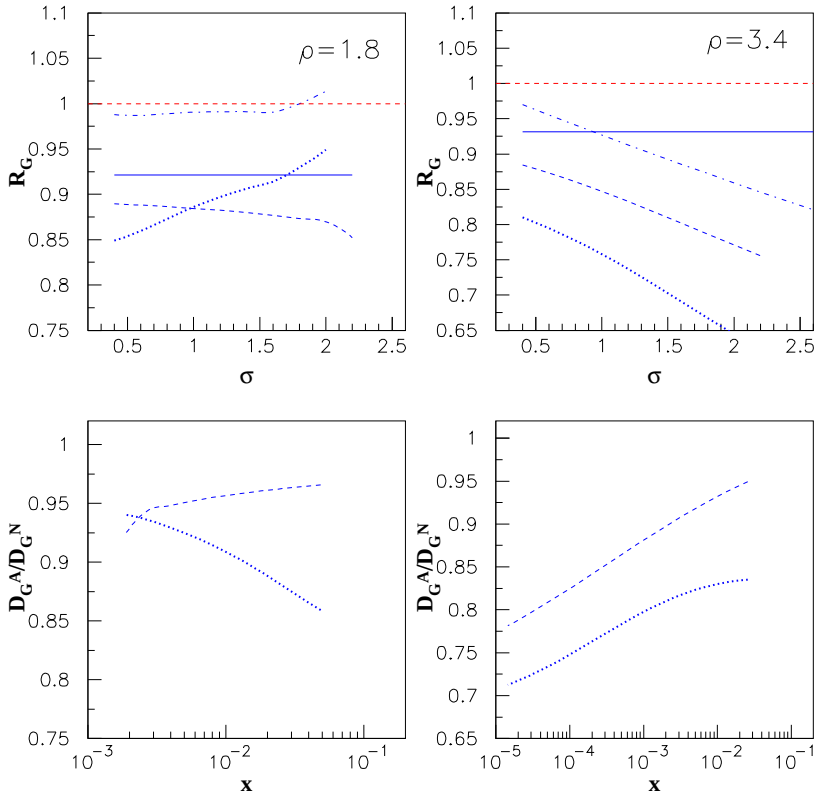

FIG. 3. Top: Ratio $R_G = G_A/G_N$, vs. DAS variable σ at two different values of ρ: $\rho = 1.8$ (left) and $\rho = 3.4$ (right). The theoretical curves show both σ-scaling (full lines) and the σ-scaling violations predicted in this paper: dashes, Eq.(15a), dots, Eq.(15b), and dot-dashes, Eq.(15c). Bottom: Ratio of nuclear to nucleon damping factors (see Eq.(14)), as a function of x for the same values of ρ and σ used in the shadowing calculations above. The Q^2 ranges are: $2.3 < Q^2 < 2 \times 10^3$ GeV^2 (left), $1.5 < Q^2 < 40.$ < GeV^2 (right). We show results using the AJM of Ref. [18] as our non-perturbative input; analogous scaling relations are found by using other initial shadowing models.